On the Rigorous Design of Graphene-based Periodic Structures Exploiting the Fundamental Resonances

Pablo H. Zapata Cano*, Stamatios Amanatiadis*, Zaharias D. Zaharis*,
Traianos V. Yioultsis*, Pavlos Lazaridis†, Nikolaos V. Kantartzis*
*School of Electrical and Computer Engineering, Aristotle University of Thessaloniki, Thessaloniki, Greece
†School of Computing and Engineering, University of Huddersfield, UK
pablozapata@auth.gr

***Abstract*—The electromagnetic response of graphene plasmonic scatterers is realized in the present work by exploiting their natural modes. Initially, a formulation to extract the latter is presented, where the planar material is modeled as an equivalent surface current. Then, a simple disk scatterer is considered and the fundamental modes are evaluated to distinguish them between edge and bulk ones, taking into account the field distribution. Moreover, the resonance frequencies for the case of incident plane-wave scattering are connected to the characteristics of the fundamental modes. Finally, a periodic array of graphene scatterers is investigated to highlight the additional plasmonic coupling resonances, corresponding to natural modes of different attributes.**

***Index Terms*—graphene, modal analysis, periodic structures, plasmons, quasinormal modes.**

I. Introduction

An exhaustive knowledge of the electromagnetic response of a resonator can serve as a powerful tool for the design of wave absorption and/or manipulation structures based on the exploitation/concatenation of their resonances. The approach of quasinormal modes (QNMs), referred, also, as fundamental or natural modes, constitutes a closed-form formulation of the local density states of the resonator [1]. They have been applied to photonic and plasmonic resonators of various geometries and materials [2], [3], and it is proved that they can accurately characterize the electromagnetic response of the system, even with a reduced number of resonance modes [4].

QNMs can be defined as electromagnetic field distributions that satisfy Maxwell's equations. For non-dispersive materials, this leads to a linear eigenproblem whose solution can be extracted efficiently with certain commercial tools. However, for the case of resonators made of dispersive materials, the problem turns to a nonlinear one, and a more complex formulation is needed to compute the QNMs and recover the electromagnetic response of the resonator [5]. Despite their higher complexity, dispersive materials constitute an attractive option due to their ability to support extraordinary characteristics, such as plasmonic resonances. Among them lies graphene which attracts the interest of the research community via its enticing mechanical, thermal, and optical characteristics, encompassing qualities such as robust electrical conductivity, and exceptional optical transparency, to name a few [6], [7].

Recently, graphene has been employed to design numerous devices in the mm-wave and low-terahertz regime, including FETs, attenuators, absorbers [8], or antennas [9]. In essence, many of these components exploit the electrically tunable conductivity of graphene, as well as its variable Fermi level or the concatenation of its plasmonic resonances to enable some functionalities, such as radio-frequency identification (RFID) or terahertz and microwave absorption. Sometimes, graphene is integrated into periodic structures made of subwavelength scatterers, benefiting from both graphene's properties and the control of the wave absorption and/or scattering achievable with the periodic arrangement of resonators. In [10], multi-mode surface plasmon resonances are exploited to design a graphene-based absorber based on dart-type single-layer graphene, whereas a flexible broadband microwave absorber with self-recoverability was fabricated with graphene sheets, as introduced in [11].

The dispersive and planar nature of graphene constitutes important challenges for the formulation of the QNMs extraction in the case of resonators composed of graphene-based materials. In a previous work [12], this is tackled by modeling graphene as an infinite conductive sheet characterized by its surface current. Moreover, and following this principle, the QNMs of a graphene-sheet resonator are extracted in [13], where the non-linearities caused by graphene in the QNMs eigenvalue problem are addressed by the formulation of a (linear) augmented space formed by the electromagnetic fields and graphene's surface current.

The present work aims to extend this formulation to the case of the QNM extraction for a simple disk plasmonic resonator. Moreover, the knowledge obtained by the QNM analysis of circular scatterers is employed to better exploit the design possibilities of periodic structures. Particularly, the effect of the coupling between resonators on the excitation via an incident plane wave is studied by means of the radar cross-section of the structure, and the extracted resonances are connected to the evaluated QNMs.

The rest of the paper is organized as follows. Section II introduces the details regarding the formulation of the QNMs problem for graphene-based resonators. Then, Section III includes the QNM analysis of a circular resonator, that is then used to form a periodic structure, whose electromagnetic performance is studied by means of the radar cross-section in Section IV. Finally, Section V contains some final remarks.

Authorized licensed use limited to: UNIVERSIDAD DE GRANADA. Downloaded on January 16,2025 at 12:03:19 UTC from IEEE Xplore. Restrictions apply.

II. QNM EXTRACTION

Graphene is modeled hereby as a 2D planar material, that can be characterized by its equivalent surface current

$$\tilde{\mathbf{J}}_{gr} = \sigma_{gr}\tilde{\mathbf{E}} \tag{1}$$

where σ_{gr} denotes the graphene's conductivity. The dispersive behavior of σ_{gr} is often described using the well-known Kubo formula, which distinguishes between intra- and inter-band contributions based on electron transitions [14]. It has been showcased that in the far-infrared regime, the intra-band contribution is dominant, which leads to the following simplified expression of σ_{gr}:

$$\sigma_{gr} = \frac{A_{\mu_c}}{j\omega + 2\Gamma_{\mathrm{gr}}} \tag{2}$$

where Γ_{gr} states for the scattering rate and, being A_{μ_c} a frequency-independent term that is related to the temperature T and the externally adjustable graphene's chemical potential μ_c as

$$A_{\mu_c} = \frac{e^2 k_B T}{\pi\hbar^2}\left[\frac{\mu_c}{k_B T} + 2\ln(e^{-\mu_c/k_B T}+1)\right] \tag{3}$$

where $\hbar$ and k_B are the Planck and Boltzmann constants, respectively, and e states for the electric charge. An advantage of this simplification of the formulation of graphene's conductivity is that it can be accurately represented by a Debye model in the aforementioned regime.

For nondispersive materials, a linear eigenvalue problem is formulated, which makes the QNMs extraction straightforward. On the other hand, when dealing with materials with frequency-dependent permeability or permittivity, the problem becomes non-linear. For this reason, the resonances of an electromagnetic system, with graphene involvement, can be defined as solutions of the source-free augmented form of Maxwell's equations [13]:

$$\begin{bmatrix} 0 & j\mu^{-1}\nabla\times & 0 \\ -j\varepsilon^{-1}\nabla\times & 0 & j\varepsilon^{-1}\delta(z) \\ 0 & -jA_{\mu_c} & j2\Gamma_{\mathrm{gr}} \end{bmatrix}\begin{bmatrix}\tilde{\mathbf{H}}_{\mathbf{m}} \\ \tilde{\mathbf{E}}_{\mathbf{m}} \\ \tilde{\mathbf{J}}_{\mathbf{m}}\end{bmatrix} = \tilde{\omega}_m \begin{bmatrix}\tilde{\mathbf{H}}_m \\ \tilde{\mathbf{E}}_{\mathbf{m}} \\ \tilde{\mathbf{J}}_{\mathbf{m}}\end{bmatrix} \tag{4}$$

where $\tilde{\boldsymbol{H}}_{\boldsymbol{m}}$ and $\tilde{\boldsymbol{E}}_{\boldsymbol{m}}$ are the magnetic and electric field, and μ and ε correspond to the material permeability and permittivity of the resonator and its surrounding environment, respectively. Moreover, $\tilde{\mathbf{J}}_{\mathbf{m}}$ corresponds to the equivalent surface current of a graphene layer at the $xy-$plane, which is ensured by the Dirac $\delta(z)$ function. Note that a $e^{j\omega t}$ dependence is assumed. In the absence of material losses, the solutions to the eigenvalue problem are "perfect" Hermitan modes (without any damping, i.e. infinite relaxation time). However, in the presence of material losses or leakage, the problem becomes non-Hermitian, and the solutions are the QNMs with complex frequency

$$\tilde{\omega}_m = \Omega_m + j\Gamma_m/2 \tag{5}$$

The real part of ω_m denotes the resonant frequency, whereas Γ_m denotes the loss rate, which is related to the mode relaxation time τ_m as $\tau_m = 1/\Gamma_m$. Large mode relaxation times correspond to narrow resonances, while short values of τ_m indicate broad resonances. This information is contained in the mode quality factor Q_m, defined as

$$Q_m = \frac{\Re(\tilde{\omega}_m)}{2\Im(\tilde{\omega}_m)} = \frac{\Omega_m}{\Gamma_m} \tag{6}$$

III. QNMS STUDY OF GRAPHENE CIRCULAR RESONATOR

The geometry of the considered resonator is depicted in Fig. 1. It consists of an infinitesimally thin circular graphene patch of radius r_s placed on the $xy-$plane. The circular shape is used due to its symmetry in terms of the resonances and the coupling between the adjacent ones.

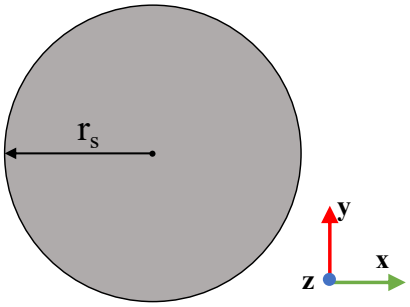

Fig. 1. Geometry of graphene circular scatterer.

The previously introduced formulation is integrated within the eigenfrequency solver of COMSOL Multiphysics [15], which allows for the calculation of the eigenfrequency and field distribution of any graphene QNM.

TABLE I
QNM EIGENFREQUENCIES FOR A CIRCULAR SCATTERER OF r_s = 40 μm

	Nature and order	**Eigenfrequency (THz)**	
		μ_c = 0.2	μ_c = 0.25
QNM 1	Edge mode 1	0.818+j0.055	0.886+j0.073
QNM 2	Edge mode 2	1.192+j0.029	1.308+j0.032
QNM 3	Edge mode 3	1.464+j0.023	1.616+j0.023
QNM 4	Bulk mode 1	1.609+j0.029	1.774+j0.032
QNM 5	Edge mode 4	1.696+j0.023	1.868+j0.022
QNM 6	Edge mode 5	1.878+j0.023	2.084+j0.022
QNM 7	Bulk mode 2	1.959+j0.029	2.172+j0.031
QNM 8	Edge mode 6	2.050+j0.022	2.278+j0.022
QNM 9	Edge mode 7	2.217+j0.028	2.455+j0.028
QNM 10	Bulk mode 3	2.222+j0.025	2.467+j0.031
QNM 11	Bulk mode 4	2.291+j0.028	2.546+j0.030
QNM 12	Edge mode 8	2.353+j0.023	2.619+j0.022
QNM 13	Bulk mode 5	2.446+j0.030	2.720+j0.030
QNM 14	Edge mode 9	2.489+j0.024	2.772+j0.023
QNM 15	Bulk mode 6	2.543+j0.028	2.830+j0.029

Authorized licensed use limited to: UNIVERSIDAD DE GRANADA. Downloaded on January 16,2025 at 12:03:19 UTC from IEEE Xplore. Restrictions apply.

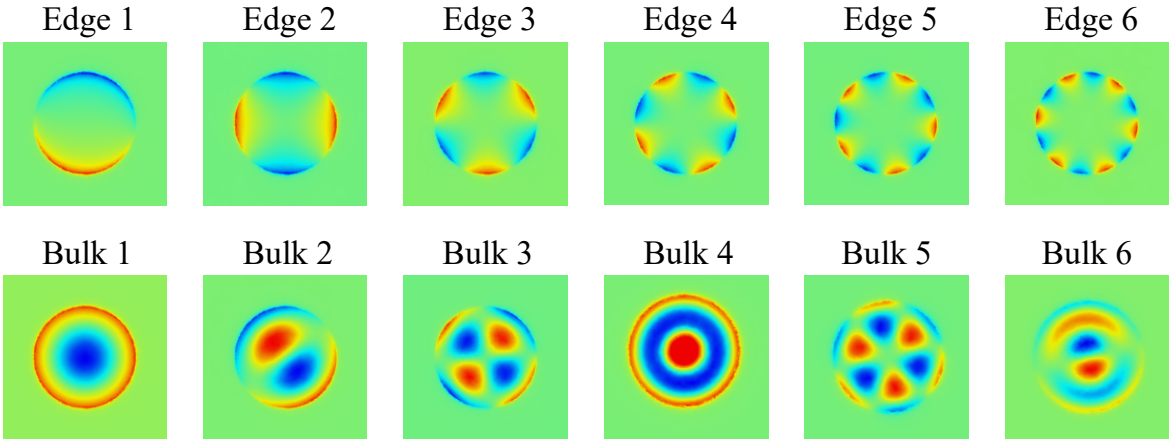

Fig. 2. Field distribution of the three first bulk and edge modes for a circular graphene patch with r_s = 40 μm and $\mu_c = 0.2$.

A list of the modes is provided in Table I at the frequency range up to 2.5 THz. QNMs can be divided into two different categories according to the nature of their field distribution. Edge modes concentrate on the patch edges, whereas bulk modes present a higher field intensity inside the surface of the graphene patch. This is illustrated in Fig. 2, where the electric field distribution of three modes of increasing order are depicted, both for bulk and edge modes.

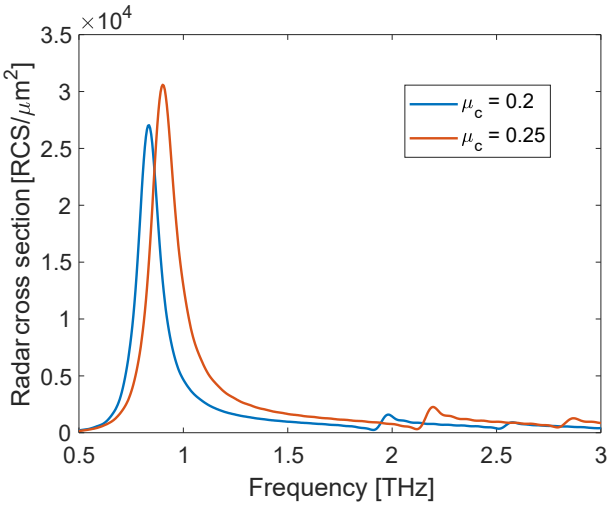

Fig. 3. RCS of single graphene circular resonator of r_s = 40 μm for two different chemical potentials.

An exhaustive knowledge of the QNMs' eigenfrequencies and nature is of big utility for a full exploitation of the structure. In the following, we consider a single graphene circular patch excited by a plane wave propagating towards the material. Then, the radar cross-section (RCS) is defined as the ratio of the scattered power to the intensity of the incident plane wave. Fig. 3 include the RCS of a circular patch between 0.5 and 1 THz for two different μ_c values, 0.2 and 0.25 eV. When μ_c is incremented from 0.2 to 0.25 eV, a similar distribution is observed but shifted to higher frequencies. Moreover, the RCS is slightly increased for the case of μ_c = 0.25. This is mainly due to the change in graphene's properties, as already predicted in [16].

Moreover, it is observed how a notable pick appears coinciding with the eigenfrequency of the first edge mode (around 0.82 THz and 0.89 THz for a chemical potential of 0.2 and 0.25, respectively). Then, two other picks are found around 2 and 2.5 THz (for a chemical potential of 0.2). It is interesting to remark that these frequencies coincide with the frequencies of the second and sixth bulk QNMs (see Table I). If we take a look at the distribution of these two modes in Fig. 2, we can see that both of them have an angular index of one, being the second mode of second order and the sixth mode of third order (radial index of 2 and 3, respectively). The same can be applied when μ_c = 0.25, which a shift in frequency.

IV. Periodic Array of Circular Resonators

In the following, the previously introduced circular scatterer is periodically arranged on the x-y plane, forming an array of resonators separated by the distance d. This geometry is illustrated in Fig. 4.

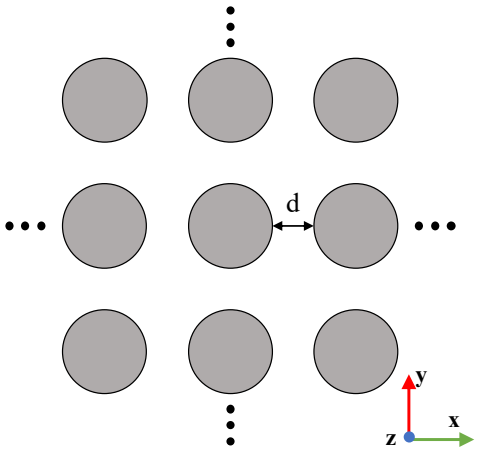

Fig. 4. Geometry of a periodic array of circular graphene resonators separated by a distance d.

Authorized licensed use limited to: UNIVERSIDAD DE GRANADA. Downloaded on January 16,2025 at 12:03:19 UTC from IEEE Xplore. Restrictions apply.

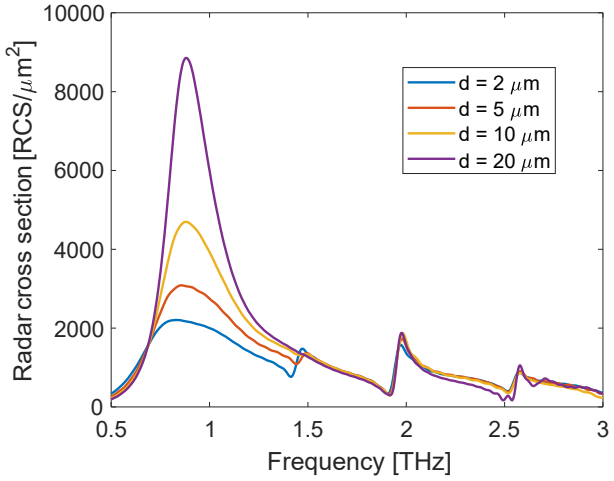

Fig. 5. Radar cross-section of a periodic array of circular resonators (r_s= 40 μm and μ_c = 0.2) as a function of the separation between them d.

In this new scenario, the coupling between resonators is added as a determinant factor for the excitation of QNMs due to the confinement of the plasmon polariton waves. In order to showcase this, the RCS is calculated for the new geometry, keeping a chemical potential of 0.2 and varying the separation between resonators d. An interesting phenomenon is that edge modes emerge, in contrast to the single scatterer case, due to the plasmonic coupling between resonators. When the period is varied, the intensity of this coupling changes, which might provoke the impedance adaptation of a different QNM, having a direct impact on the RCS. This is the case for some edge modes in Fig. 5. A pick in the RCS starts to emerge around 1.48 THz as the separation d is decreased. This coincides with the resonant frequency of the third edge mode (see Table I). Moreover, the same phenomenon might occur around 1.2 THz for the second edge mode. However, this would not be visible in the RCS due to the closeness in frequency to the wide pick provoked by the first edge mode.

V. Conclusion

Throughout this work, a formulation to extract the quasinormal modes of graphene-based resonators is presented, in which graphene is modeled as a planar material characterized by its equivalent surface current. This formulation is then employed to perform an analysis of the natural resonances of a circular scatterer between 0.8 and 2.5 THz. The contribution of the different QNMs on the radar cross-section is analyzed both for the case of a single scatterer and a periodic structure. Conclusions about the nature of the modes having an impact on the RCS and the effect of the variation of the period are made, which can serve as guidelines for the design of absorption/wave manipulation devices using this geometry.

Acknowledgment

This research was supported by the European Union, through the Horizon 2020 Marie Skłodowska-Curie Innovative Training Networks Programme “Mobility and Training for beyond 5G Ecosystems (MOTOR5G)” under grant agreement no. 861219.

References

[1] C. Sauvan, J. P. Hugonin, I. S. Maksymov, and P. Lalanne, “Theory of the spontaneous optical emission of nanosize photonic and plasmon resonators,” *Physical Review Letters*, vol. 110, 6 2013.

[2] C. Forestiere, G. Miano, M. Pascale, and R. Tricarico, “Electromagnetic scattering resonances of quasi-1-d nanoribbons,” *IEEE Transactions on Antennas and Propagation*, vol. 67, no. 8, pp. 5497–5506, 2019.

[3] L. Huang, L. Xu, D. A. Powell, W. J. Padilla, and A. E. Miroshnichenko, “Resonant leaky modes in all-dielectric metasystems: Fundamentals and applications,” *Physics Reports*, vol. 1008, pp. 1–66, 2023.

[4] P. Lalanne, W. Yan, K. Vynck, C. Sauvan, and J. P. Hugonin, “Light interaction with photonic and plasmonic resonances,” 5 2018.

[5] P. Lalanne, W. Yan, A. Gras, C. Sauvan, J.-P. Hugonin, M. Besbes, G. Demésy, M. D. Truong, B. Gralak, F. Zolla, A. Nicolet, F. Binkowski, L. Zschiedrich, S. Burger, J. Zimmerling, R. Remis, P. Urbach, H. T. Liu, and T. Weiss, “Quasinormal mode solvers for resonators with dispersive materials,” *Journal of the Optical Society of America A*, vol. 36, p. 686, 4 2019.

[6] G. W. Hanson, “Dyadic green’s functions for an anisotropic, non-local model of biased graphene,” *IEEE Transactions on Antennas and Propagation*, vol. 56, pp. 747–757, 3 2008.

[7] Y. Zhu, S. Murali, W. Cai, X. Li, J. W. Suk, J. R. Potts, and R. S. Ruoff, “Graphene and graphene oxide: Synthesis, properties, and applications,” *Advanced Materials*, vol. 22, pp. 3906–3924, 9 2010.

[8] C. Fu, L. Zhang, L. Liu, S. Dong, W. Yu, and L. Han, “Rcs reduction on patterned graphene-based transparent flexible metasurface absorber,” *IEEE Transactions on Antennas and Propagation*, vol. 71, no. 2, pp. 2005–2010, 2023.

[9] G. C. Ghivela and J. Sengupta, “The promise of graphene: A survey of microwave devices based on graphene,” *IEEE Microwave Magazine*, vol. 21, pp. 48–65, 2020.

[10] H. Chen, Z. Chen, H. Yang, L. Wen, Z. Yi, Z. Zhou, B. Dai, J. Zhang, X. Wu, and P. Wu, “Multi-mode surface plasmon resonance absorber based on dart-type single-layer grapheme,” *RSC Advances*, vol. 12, pp. 7821–7829, 3 2022.

[11] K. L. Zhang, J. Y. Zhang, Z. L. Hou, S. Bi, and Q. L. Zhao, “Multifunctional broadband microwave absorption of flexible graphene composites,” *Carbon*, vol. 141, pp. 608–617, 2019. [Online]. Available: https://doi.org/10.1016/j.carbon.2018.10.024

[12] P. H. Cano, S. Amanatiadis, Z. D. Zaharis, T. V. Yioultsis, P. I. Lazaridis, and N. V. Kantartzis, “Robust fdtd modeling of graphene-based conductive materials with transient features for advanced antenna applications,” *Nanomaterials*, vol. 13, 2 2023.

[13] S. Amanatiadis, T. Ohtani, T. Zygiridis, Y. Kanai, and N. Kantartzis, “Effective finite-difference modeling of graphene micro-resonators for the accurate natural frequency extraction,” *IEEE Transactions on Magnetics*, pp. 1–1, 9 2023.

[14] G. W. Hanson, “Dyadic green’s functions and guided surface waves for a surface conductivity model of graphene,” *Journal of Applied Physics*, vol. 103, 2008.

[15] “COMSOL Multiphysics,” COMSOL AB: Stockholm, Sweden, 2022.

[16] M. Lucido, “Electromagnetic scattering from a graphene disk: Helmholtz-galerkin technique and surface plasmon resonances,” *Mathematics*, vol. 9, 6 2021.

Authorized licensed use limited to: UNIVERSIDAD DE GRANADA. Downloaded on January 16,2025 at 12:03:19 UTC from IEEE Xplore. Restrictions apply.